THE JOURNAL OF BIOLOGICAL CHEMISTRY
Vol. 278, No. 48, Issue of November 28, pp. 47997–48003, 2003
Printed in U.S.A.

Modeling β-Adrenergic Control of Cardiac Myocyte Contractility *in Silico**

Received for publication, July 30, 2003, and in revised form, September 10, 2003
Published, JBC Papers in Press, September 12, 2003, DOI 10.1074/jbc.M308362200

Jeffrey J. Saucerman‡, Laurence L. Brunton§, Anushka P. Michailova‡¶, and Andrew D. McCulloch‡‖

From the ‡Department of Bioengineering, University of California, San Diego, La Jolla, California 92093-0412, the §Department of Pharmacology, University of California, San Diego, La Jolla, California 92093-0636, and the ¶Department of Biophysics, Bulgarian Academy of Science, 1113 Sofia, Bulgaria

The β-adrenergic signaling pathway regulates cardiac myocyte contractility through a combination of feedforward and feedback mechanisms. We used systems analysis to investigate how the components and topology of this signaling network permit neurohormonal control of excitation-contraction coupling in the rat ventricular myocyte. A kinetic model integrating β-adrenergic signaling with excitation-contraction coupling was formulated, and each subsystem was validated with independent biochemical and physiological measurements. Model analysis was used to investigate quantitatively the effects of specific molecular perturbations. 3-Fold overexpression of adenylyl cyclase in the model allowed an 85% higher rate of cyclic AMP synthesis than an equivalent overexpression of β_1-adrenergic receptor, and manipulating the affinity of $G_s\alpha$ for adenylyl cyclase was a more potent regulator of cyclic AMP production. The model predicted that less than 40% of adenylyl cyclase molecules may be stimulated under maximal receptor activation, and an experimental protocol is suggested for validating this prediction. The model also predicted that the endogenous heat-stable protein kinase inhibitor may enhance basal cyclic AMP buffering by 68% and increasing the apparent Hill coefficient of protein kinase A activation from 1.0 to 2.0. Finally, phosphorylation of the L-type calcium channel and phospholamban were found sufficient to predict the dominant changes in myocyte contractility, including a 2.6× increase in systolic calcium (inotropy) and a 28% decrease in calcium half-relaxation time (lusitropy). By performing systems analysis, the consequences of molecular perturbations in the β-adrenergic signaling network may be understood within the context of integrative cellular physiology.

In the cardiac myocyte, the β-adrenergic signaling network responds to the catecholamines norepinephrine and epinephrine, providing coordinated control of contractility, metabolism, and gene regulation (1, 2). These actions are initiated by β-adrenergic receptor coupling with G_s and subsequent stimulation of adenylyl cyclase, which synthesizes the classical second messenger cyclic AMP. Cyclic AMP promotes dissociation of the protein kinase A (PKA)[1] holoenzyme, whose catalytic subunits phosphorylate a wide spectrum of target proteins. The β-adrenergic control of cardiac contractility is believed to be dominated by PKA phosphorylation of the L-type calcium channel and phospholamban (3), important players in the regulation of calcium dynamics and transport. Although this network mediates the contractile response to catecholamines in the healthy myocyte, altered β-adrenergic signaling may also play an incompletely understood role in the progression of heart failure (1, 3).

Modules in this network have received considerable attention as possible therapeutic targets in congestive heart failure, including β-receptors, adenylyl cyclase (4), and phospholamban (5). Recent studies (6–8) suggest an important role of compartmentation in signaling specificity. Whereas fluorescent probes (9–11) and biophysical measurements (5, 12) allow dynamic responses to be recorded in intact cells, the growing complexity of signaling networks complicates the intuitive interpretation of observed physiological responses in terms of the underlying molecular processes.

To probe the functional interactions of signaling networks in the context of integrative cellular physiology, systems level modeling and analysis will be valuable. Because the work of Hodgkin and Huxley in 1952 (13), ionic models of cell electrophysiology have complemented experimental research and helped in the formulation of new biological hypotheses (14). Recent large scale efforts such as the Alliance for Cellular Signaling have identified systems modeling as essential for a comprehensive understanding of signaling networks and the response to genetic and pharmacological perturbations (15).

Whereas portions of the mammalian β-adrenergic signaling network have been modeled mathematically in neurons and HEK-293 cells (16, 17), no analysis has modeled and validated an entire pathway from ligand to effectors so that neurohormonal regulation of cell physiology can be predicted. Here we use a systems model to investigate how the topology and interacting components in the β-adrenergic signaling network contribute to the control of cardiac myocyte contractility. Validation against a wide range of independent experimental data

* This work was supported by National Biomedical Computation Resource Grant P41 RR08605 (to A. D. M.), National Space Biomedical Research Institute Project CA00216 (to A. D. M.), National Science Foundation Grant BES-0096482 (to A. D. M.), NHLBI Grant HL-41307 (to L. L. B.) from the National Institutes of Health, National Institutes of Health Grant 5 P50 HL53773-09 (to K. R. Chien), and a Whitaker Foundation Graduate fellowship (to J. J. S.). The costs of publication of this article were defrayed in part by the payment of page charges. This article must therefore be hereby marked "*advertisement*" in accordance with 18 U.S.C. Section 1734 solely to indicate this fact.

[S] The on-line version of this article (available at http://www.jbc.org) contains Appendices A and B and additional Refs. 1–34.

‖ To whom correspondence should be addressed: Dept. of Bioengineering, University of California, San Diego, 9500 Gilman Dr., La Jolla, CA 92093-0412. Tel.: 858-534-2547; Fax: 858-534-6896; E-mail: amcculloch@ucsd.edu.

[1] The abbreviations used are: PKA, protein kinase A; GTPγS, guanosine 5′-3-*O*-(thio)triphosphate; Gpp(NH)p, guanosine 5′-(β,γ-imido)triphosphate; AC, adenylyl cyclase; PLB, phospholamban; LCC, L-type calcium channel; IBMX, 3-isobutyl-1-methylxanthine; SR, sarcoplasmic reticulum; PKI, protein kinase inhibitor.

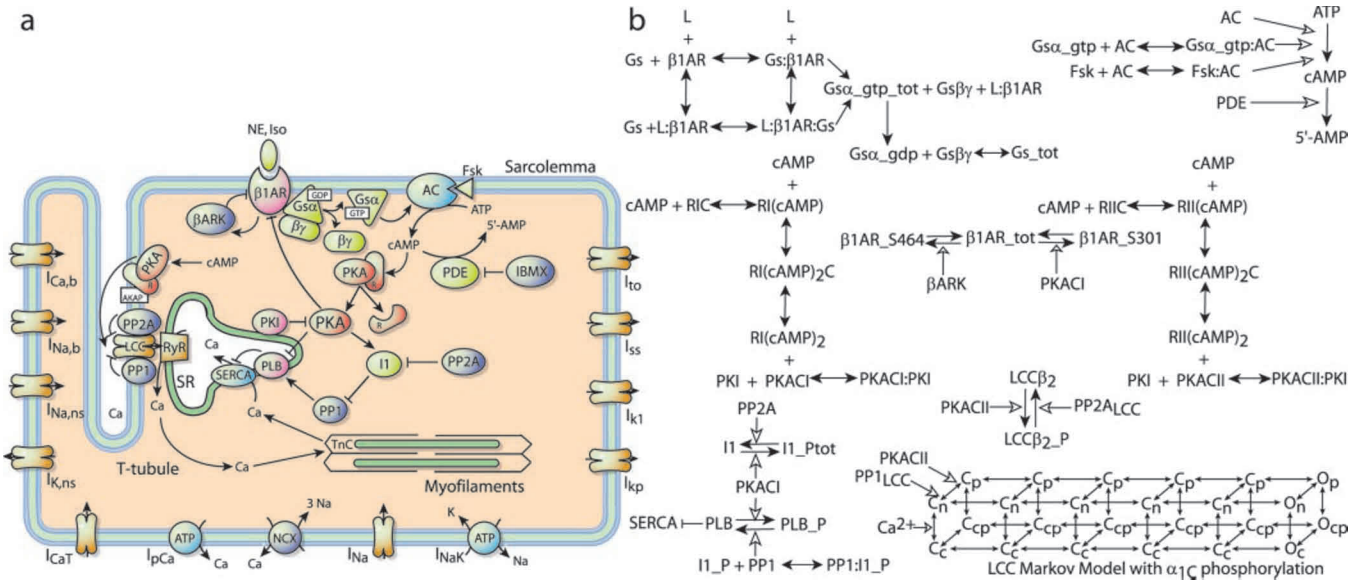

FIG. 1. **Schematics of the β-adrenergic network and signaling mechanisms in the model.** *a*, schematic of integrated model components, including the β_1-adrenergic network, calcium handling, and electrophysiology of the rat ventricular myocyte. *b*, network topology and reaction mechanisms in the β-adrenergic signaling model. *Single-headed filled arrows* denote kinetics; *single-headed empty arrows* denote enzyme catalysis, and *double-headed arrows* denote quasi-equilibrium reactions. *NE*, norepinephrine; *Iso*, isoproterenol; *β_1-AR*, β_1-adrenergic receptor; *βARK*, β-adrenergic receptor kinase; *AC*, adenylyl cyclase; *Fsk*, forskolin; *PDE*, phosphodiesterase; *PKA*, protein kinase A; *RIC/RIIC*, type I/II PKA holoenzyme (*b* only); *PKI*, heat-stable protein kinase inhibitor; *PP1*, protein phosphatase-1; *PP2A*, protein phosphatase-2A; *I1*, inhibitor-1; *PLB*, phospholamban; *LCC*, L-type calcium channel; *SERCA*, sarcoplasmic reticulum Ca^{2+}-ATPase; *RyR*, ryanodine receptor.

including cyclic AMP, phosphorylation, and calcium and electrophysiological assays demonstrate excellent consistency on a number of functional levels. The kinetic model was used to perform systematic *in silico* perturbations to the β-adrenergic network, whose interpretations show potential in molecular therapeutic analysis, experimental design, and the identification of signaling control mechanisms. These systems analyses provide a framework for a more integrated understanding of the β-adrenergic signaling mechanisms that control cardiac myocyte contractility.

EXPERIMENTAL PROCEDURES

A differential algebraic model of β_1-adrenergic signaling in the cardiac myocyte was formulated using the singular perturbation method (18), which decomposed the network into characteristic time scales. Sub-networks with dynamics on very fast time scales (<0.1 s) were assumed to be at quasi-equilibrium (*e.g.* binding reactions) and represented by algebraic equations, whereas sub-networks with very slow dynamics (>10 min) were assumed to be time-invariant (*e.g.* receptor internalization and gene expression). Remaining differential equations utilized standard rate laws such as mass action and Michaelis-Menten kinetics. Examples of differential and algebraic equations from the model are shown below, describing the rate of change of total GTP-bound $G_s\alpha$ (Eq. 1) and the amount of GTP-bound $G_s\alpha$ that is bound transiently to adenylyl cyclase (Eq. 2),

$$\frac{d([G_s\alpha_{GTPtot}])}{dt} = k_{gact}([RG] + [LRG]) - k_{hyd}[G_s\alpha_{GTPtot}] \quad \text{(Eq. 1)}$$

$$[G_s\alpha_{GTPtot}] - [G_s\alpha_{GTP}] - [G_s\alpha_{GTP}{:}AC] = 0 \quad \text{(Eq. 2)}$$

Parameters were obtained from the literature whenever possible and generally measured *in vitro* with purified components or measured in rat ventricular myocytes (56 parameters). The remaining parameters were constrained using independent experimental data from the literature (11 parameters). The signaling network consisted of 37 differential and 12 algebraic equations. All equations and parameters from the signaling network model are provided in the Supplemental Material.

Recent experimental techniques have enabled quantification of signaling specificity and speed afforded by protein complexation and scaffolding (10, 19). To capture the essence of these results within a traditional framework, we have introduced a coefficient ϵ, which modifies the effective concentration of proteins for reactions between members of a protein complex or microdomain, where $[X]_{effective} = \epsilon\,[X]$. This coefficient can be measured experimentally as the ratio of time constants without and with complexation, or $\epsilon = \tau_{free}/\tau_{cmplx}$. For the current model, a constant value of $\epsilon = 10$ was used, based on fluorescence resonance energy transfer experiments used in conjunction with flash photolysis of caged cyclic AMP (10). This approach was used to model localization of type II PKA, protein phosphatase-1, and protein phosphatase-2A to the LCC and protein phosphatase-1 to PLB.

The calcium handling and electrophysiology portion of the model was based on an extension of the Luo-Rudy model (20), modified for the rabbit ventricular myocyte (LabHEART) (21). Here this model was adapted to simulate the rat ventricular myocyte using experimental calcium handling data (3) and previously described formulations for the L-type calcium channel (22), transient outward, and steady-state potassium currents (23). The resulting model was stable and exhibited positive excitation-contraction coupling gain and a negative force-frequency relationship (not shown), as seen experimentally in rat ventricular myocytes (3). The complete signaling, calcium handling, and electrophysiology model was implemented with the Rosenbrock stiff solver in Berkeley Madonna (www.berkeleymadonna.com).

RESULTS

Formulation and Validation of Functionally Integrated Models—We developed a kinetic model of β-adrenergic signaling, calcium handling, and electrophysiology in the cardiac myocyte (Fig. 1). Briefly, the model describes agonist stimulation of β_1-adrenergic receptor, activation of G_s protein, cyclic AMP synthesis by AC, cyclic AMP degradation by phosphodiesterase, PKA subunit activation and dissociation, phosphorylation of important target proteins phospholamban (PLB) and the L-type calcium channel (LCC), and β-adrenergic receptor kinase and PKA-mediated β_1-adrenergic receptor desensitization.

Type I PKA, the dominant PKA in the rat ventricular myocyte, diffuses throughout the cytosol. A population of A kinase anchoring protein-bound type II PKA is localized near the L-type calcium channel, along with a fraction of protein phosphatase-1 and protein phosphatase-2A (3). Control of the SR Ca^{2+}-ATPase by PLB is achieved by regulating the Ca^{2+} affinity of the pump, whereas control of the LCC is achieved by regulating channel availability and a state transition that affects channel open probability. As shown in Fig. 1*a*, PLB and LCC act as key connections between β-adrenergic signaling and excitation-contraction coupling in the model. The specific

reaction schemes modeled are shown in Fig. 1*b*, with *single-headed filled arrowheads* denoting kinetics, *single-headed empty arrowheads* denoting enzyme catalysis, and *double-headed arrowheads* denoting quasi-equilibrium reactions. For example, PKA-mediated phosphorylation of β_1-adrenergic receptor to β_1-AR_S301 is modeled kinetically (*single-headed filled arrowheads*) with facilitation by PKA (*single-headed empty arrowheads*). On the other hand, ligand (L) binding to β_1-adrenergic receptor to form the complex L·β_1-adrenergic receptor is modeled as a quasi-equilibrium reaction, which has *double-headed filled arrowheads.* Integrated with a model of rat ventricular myocyte calcium handling and electrophysiology, the functional role of these signaling networks can be investigated.

The model was validated with a wide range of experimental data (plotted as *circles*) from the literature (Fig. 2). The model reproduces the temporal response to β-adrenergic agonist isoproterenol with partial adaptation due to desensitization (Fig. 2*a*) (9, 24) over a wide range of agonist concentrations (Fig. 2*b, dashed line*). When phosphodiesterase is inhibited so that cyclic AMP accumulation is a more direct measure of AC activity (Fig. 2*b*), cyclic AMP accumulation in the model (*solid line*) agrees well with experimental data (*filled circles*) with 3-isobutyl-1-methylxanthine (IBMX) (25). Tests of PKA activation (Fig. 2, *c* and *d*) with (*dotted line*) and without (*solid line*) the heat-stable protein kinase inhibitor (PKI) demonstrate a cyclic AMP-stimulated activation/dissociation relationship consistent with experimental data (*circles*) measured at physiological PKA concentrations (26). Numerical experiments also show consistent relationships between agonist concentration and phosphorylation targets, particularly PLB phosphorylation (Fig. 2*e*) (27) and single channel measurements of the LCC such as channel availability and open probability (not shown). Finally, the entire functionally integrated model was validated against measured changes in whole cell patch-clamped calcium currents (Fig. 2*f*), calcium transients (Fig. 2*g*), and action potential (Fig. 2*h*) in response to 1 μM isoproterenol (*dotted lines*) (3, 28, 29). Isoproterenol stimulation causes an increase in calcium transient magnitude (control, 0.66 μM, *versus* isoproterenol, 1.71 μM), a decrease in diastolic calcium concentration (control, 0.14 μM, *versus* isoproterenol, 0.10 μM), a decrease in half-relaxation time $t_{½}$ of the calcium transient (control, 117 ms, *versus* isoproterenol, 85 ms), an increase in SR Ca^{2+} load (control, 96 μmol/liter cytosol, *versus* isoproterenol, 168 μmol/liter cytosol), and an increase in APD80 (control, 30 ms, *versus* isoproterenol, 42 ms). These results represent stringent tests of model consistency, providing confidence in the utility of the model for generating and testing biological hypotheses.

Analysis of Potential and Novel Molecular Therapeutics—A number of potential gene therapies have been proposed to modify β-adrenergic signaling at the receptor or adenylyl cyclase level, and these efforts have seen some success in animal models of heart failure (4). However, these approaches are hindered by difficulties in predicting the systemic effects of an acute perturbation and systematically identifying potential alternatives. Cellular systems modeling may serve as a useful tool for analysis and design of molecular therapeutics.

Here we compare model analyses of receptor overexpression, adenylyl cyclase overexpression, and a novel potential pharmacological alternative. This alternative therapy, motivated by model analysis, involves increasing the affinity for $G\alpha_s$-GTP and adenylyl cyclase ($1/K_{Gs\alpha}$), similar to the action of forskolin. The ability of 3-fold increases in AC expression (Fig. 3*a*, *dashed line*), β_1-adrenergic receptor expression (*dotted line*), and α_s-GTP/AC affinity (*dashed-dotted line*) to affect isoproterenol-stimulated adenylyl cyclase activity was assessed in the presence of 1 mM IBMX. In addition, equipotent (as determined as in Fig. 3*a*) treatments (Fig. 3*b*; 1.5× AC, *dashed line*; 1.8× β_1-adrenergic receptor, *dotted line*; 1.9× $1/K_{Gs\alpha}$, *dashed-dotted line*) were tested for the undesired side effect of increased basal cyclic AMP content, which may lead to a hypertrophic response (4). Equipotent treatments appeared to elevate basal cyclic AMP content similarly. The results from Fig. 3, *a* and *b*, are qualitatively consistent with experimental data from transgenic mice overexpressing AC5 or β-adrenergic receptor (30, 31).

When comparing equal magnitude treatments (3-fold overexpression or 3-fold increase in affinity), adenylyl cyclase overexpression appears to be the most effective at increasing isoproterenol response with minimal side effects. Although

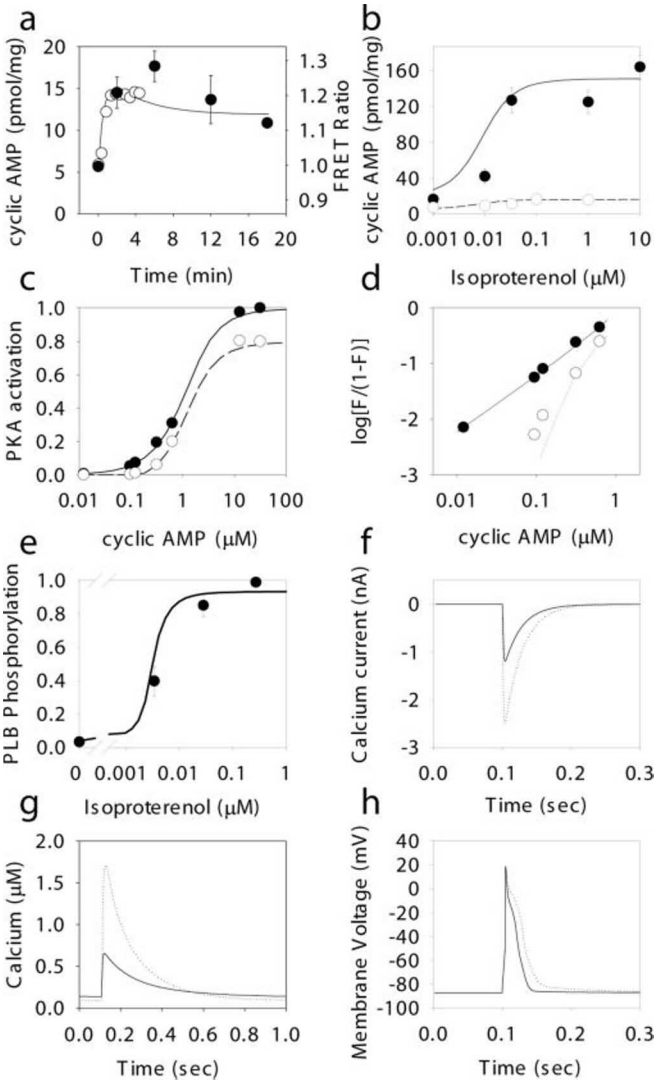

FIG. 2. **Experimental validation.** *a*, temporal response of cyclic AMP accumulation to 10 nM isoproterenol. *b*, concentration dependence of cyclic AMP accumulation to isoproterenol, with (*solid line*) and without (*dashed line*) 0.1 mM phosphodiesterase inhibitor IBMX. *c*, concentration dependence of PKA activation to cyclic AMP, with (*dashed line*) and without (*solid line*) 60 nM PKI. *d*, Hill plot of PKA activation with (*dotted line*) and without (*solid line*) PKI, where *f* is the fraction of PKA activation (same data as *c*). *e*, concentration dependence of phospholamban phosphorylation to isoproterenol. *f*, whole cell patch-clamped calcium current (holding potential at −80 mV, step to 0 mV) with (*dotted line*) and without (*solid line*) 1 μM isoproterenol. *g*, calcium transient and *h* action potential (1 Hz) with (*dotted line*) and without (*solid line*) 1 μM isoproterenol. Results in *a–e* show direct comparison with published experimental data (*filled* or *empty circles*) (9, 24–27), whereas results in *f–h* are consistent with experimental measurements (3, 28, 29).

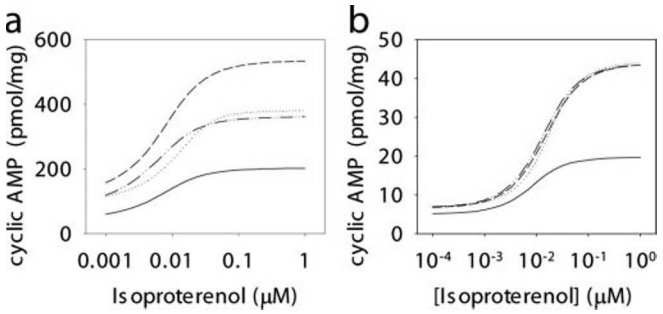

FIG. 3. ***In silico*** **analysis of molecular therapeutics for heart failure.** *a*, concentration dependence of cyclic AMP accumulation to isoproterenol in control (*solid line*), 3× AC overexpression (*dashed*), 3× β_1-adrenergic receptor overexpression (*dotted*), and 3× $1/K_{Gs\alpha}$ (affinity of $G\alpha_s$-GTP for AC; *dashed-dotted*) treatments, demonstrating efficacy of each therapy at increasing the response to agonist. All runs performed with 1 mM IBMX. *b*, concentration dependence of cyclic AMP accumulation to isoproterenol in control (*solid line*) and equipotent treatments: 1.5× AC overexpression (*dashed line*), 1.8× β_1-adrenergic receptor overexpression (*dotted line*), and 1.9× $1/K_{Gs\alpha}$ (*dashed-dotted line*), demonstrating the effects of proposed treatments on basal cyclic AMP content. Treatments are generally designed to maximize isoproterenol response while maintaining a physiological basal cyclic AMP content. Results are qualitatively consistent with experimental data from transgenic mice overexpressing AC5 or β-adrenergic receptor (30, 31).

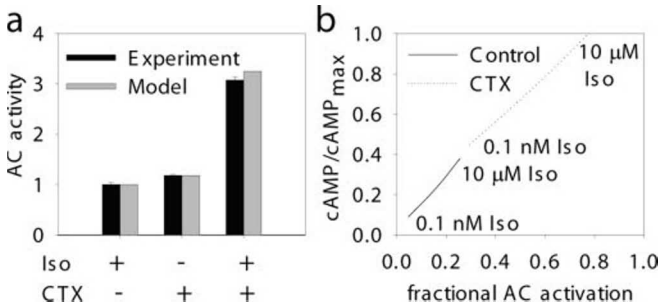

FIG. 4. **Experimental design, using cholera toxin (*CTX*) to estimate fractional AC activation.** *a,* cyclic AMP response to 1 μM isoproterenol (*Iso*) with and without 300 ng/ml cholera toxin (*gray bars*), compared with experimental data (*black bars*) (34). *b,* linear relationship between fractional AC activation and cyclic AMP accumulation, when measured using 1 mM IBMX at 3 min and normalizing cyclic AMP accumulation to an experiment measuring cyclic AMP maximally stimulated by isoproterenol and cholera toxin. Note the small range of physiological fractional AC activation in the absence of cholera toxin (*solid line*).

greater receptor overexpression is possible, this comes at the cost of intolerably high basal cyclic AMP content due to constitutively activated receptors and other undesired effects. Increasing the affinity of $G_s\alpha$ and adenylyl cyclase by pharmacological means seems to have an effect similar to receptor overexpression. Such a strategy may have some advantages: 1) small molecule agents may be preferred to gene therapy, 2) lead optimization can be used to fine-tune the properties of the drug, and 3) the drug may be specifically targeted to certain microdomains, using compartmentation to minimize undesired increase in basal cyclic AMP content (Fig. 3*b*). Although a thorough consideration of compartmentation and cross-talk with other pathways may be required for a more comprehensive understanding, this analysis demonstrates the potential for models in analyzing the design goals and tradeoffs presented by many alternative therapeutic targets.

Model-driven Experimental Design—Systems models present opportunities to design new experiments and formulate novel hypotheses, as illustrated recently by Hoffmann *et al.* (32). By using our model, we demonstrate a simple experimental design to estimate the fractional activation of adenylyl cyclase, which may prove to be useful in understanding the mechanisms by which cyclic AMP signaling is controlled.

Whereas adenylyl cyclase has been described as stoichiometrically limiting in cyclic AMP metabolism (33) (motivating target selection for gene therapy), preliminary modeling indicated that under physiological conditions only a small fraction of adenylyl cyclase may be activated. This paradoxical result suggests that receptor overexpression and the novel pharmacological therapy proposed above may function by increasing the fraction of adenylyl cyclase molecules that bind $G_s\alpha$. A physiologically low fractional adenylyl cyclase activation is consistent with the finding that very high receptor overexpression levels are able to maximally stimulate adenylyl cyclase (31). Lacking methods to measure fractional adenylyl cyclase activation experimentally, we have designed a protocol to estimate this quantity indirectly, and we show that simulated results are linearly proportional to the actual fractional activation of adenylyl cyclase, suggesting a useful experimental protocol.

This strategy would take advantage of the ability of cholera toxin to prevent the hydrolysis of GTP from $G_s\alpha$ or the resistance to hydrolysis of synthetic derivatives GTPγS and Gpp(NH)p. In Fig. 4*a*, the cyclic AMP response to 1 μM isoproterenol with and without reduced GTP hydrolysis is successfully validated with experimental data from Chung *et al.* (34). Agonist-stimulated activation of $G_s\alpha$, coupled with the prevention of GTP hydrolysis by cholera toxin, keeps a large amount of $G_s\alpha$ in the GTP-bound state, causing near-maximal fractional activation of available adenylyl cyclase molecules (here 90% before desensitization).

These results suggest that one could estimate fractional AC activation with a simple protocol involving cholera toxin. Positive control cells are given a maximally effective (~300 ng/ml) dose of cholera toxin and nonspecific phosphodiesterase inhibitor IBMX (~1 mM) together with a high concentration of agonist (~10 μM isoproterenol). The experiment is terminated at 3 min to minimize the effect of receptor desensitization, and cyclic AMP is measured to determine the AC activity at maximal fractional AC activation. In parallel, the protocol is performed with or without cholera toxin and various doses of agonist or other pharmacological agents to compare with the positive control. By normalizing the measured cyclic AMP for each run by the results from the positive control (agonist + cholera toxin), an index of AC activation is obtained that correlates closely with the true fractional AC activation.

We performed a numerical experiment to test whether a good estimate of fractional AC activation would be obtained with the above protocol (Fig. 4*b*). Over a wide range of agonist concentrations (0.1 nM to 10 μM isoproterenol) with (*dotted line*) and without (*solid line*) cholera toxin, we found a linear relationship between fractional AC activation and the normalized cyclic AMP accumulation. Fig. 4*b* demonstrates that in physiological conditions, fractional activation of AC at 3 min may be limited to a range between 5 and 26%, with a maximum activation of less than 40%. This finding suggests a possible role for currently uncharacterized natural or synthetic regulatory molecules to increase AC stimulation.

Control Mechanisms in Cyclic AMP and Calcium Signaling—Whereas β-adrenergic signaling in the cardiac myocyte is one of the best characterized of mammalian signaling networks, the systems model presents an opportunity for analyses that may be difficult to predict or measure experimentally. The model is especially useful for predicting the effects of molecular interventions on a systems level relevant to whole cell function.

To examine the role of cyclic AMP buffering in cellular function, we examined the concentration dependence of cyclic AMP to isoproterenol in control (Fig. 5, *solid line*), PKA knockout

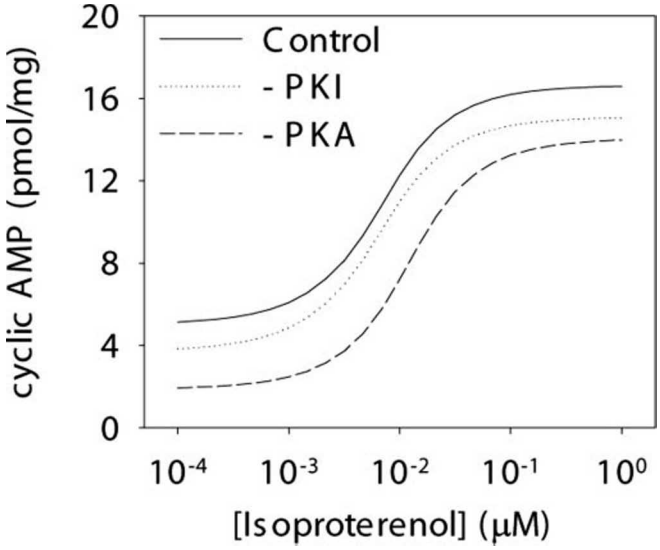

FIG. 5. **Role of cyclic AMP buffering by PKA and the heat-stable PKI.** Dose response of cyclic AMP to isoproterenol in control (*solid line*), PKI knockout (*−PKI*; *dotted line*), and PKA knockout (*−PKA*; *dashed line*) models. Both PKA and PKI contribute significantly to cyclic AMP buffering at low stimulus levels, maintaining basal cyclic AMP levels. Due to network topology, the action of PKI requires the presence of PKA.

(*−PKA*; *dashed line*), and PKI knockout (*−PKI*; *dotted line*) versions of the model. Whereas PKA is known to be a significant cyclic AMP buffer and the primary mediator of cyclic AMP effects in the cell, the physiological role of the heat-stable protein kinase inhibitor (PKI) is not well characterized. As expected, comparison of the control and PKA knockout reveals significant buffering (the difference between the *solid* and *dashed lines*) over the entire range of isoproterenol concentrations due to PKA. More interesting is the indirect role of PKI in cyclic AMP buffering at low agonist concentrations (Fig. 5, compare *solid* and *dotted lines*), achieved by shifting the equilibrium of PKA activation toward greater holoenzyme dissociation and cyclic AMP retention (see reaction diagram in Fig. 1*b*). Additionally, PKI significantly increases the apparent Hill coefficient of PKA activation (from $n = 1.0–2.0$; Fig. 2*c*), a phenomenon known as ultrasensitivity due to a stoichiometric (high affinity) inhibitor (35).

Whereas buffering of cyclic AMP by PKA and regulation of buffering by PKI helps maintain the amount of bound cyclic AMP in the cell (Fig. 5), the free cyclic AMP concentration is more sensitive to the balance of AC and phosphodiesterase activities and relatively insensitive to the presence of cyclic AMP buffers (not shown). These results provide a new perspective on the functional role of cyclic AMP buffering, in that buffering may provide a mechanism for maintaining a basal bound cyclic AMP content that is relatively insensitive to changes in synthesis (AC) and degradation (phosphodiesterase) activities. On the cellular level, cyclic AMP buffering may help maintain the basal phosphorylation state of PKA targets and enable prompt response to sympathetic stimulation via the β-adrenergic receptor.

Examining the broader roles of cyclic AMP signaling, we explore the control of calcium handling mediated by phosphorylation of the L-type calcium channel and phospholamban. A steady-state (1 Hz) calcium transient in an isoproterenol-stimulated cell was computed (Fig. 6*a*; *PLB + LCC, solid line*), together with variations in which only LCC (*dotted line*) or PLB (*dashed line*) can be phosphorylated. This analysis allows the contribution of each target to be distinguished, which would be difficult to measure experimentally. Whereas LCC and PLB

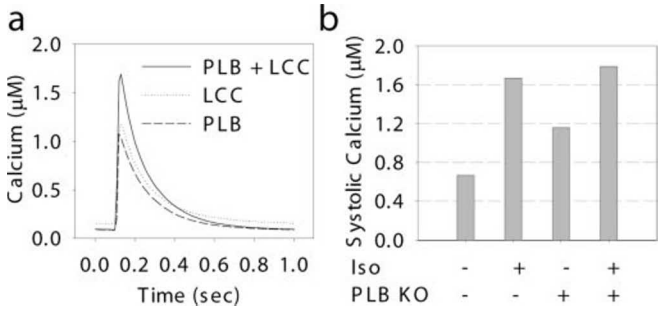

FIG. 6. **Role of the LCC and PLB phosphorylation in myocyte calcium handling.** *a*, calcium transient in isoproterenol-stimulated cells: normal (*solid line*), LCC phosphorylation only (*dotted line*), and PLB phosphorylation only (*dashed line*). *b*, response of calcium transient magnitude to isoproterenol, both in control and PLB knockout (*PLB KO*) models, consistent with experimental data (3).

phosphorylation appear to have similar effects on the magnitude of the calcium transient (PLB, 1.07 μM, *versus* LCC, 1.17 μM; Fig. 6*a*), PLB appears to be largely responsible for changes in diastolic calcium (PLB, 0.09 μM, *versus* LCC, 0.15 μM), half-relaxation time $t_{1/2}$ (PLB, 101 ms, *versus* LCC, 109 ms), and SR Ca^{2+} load (PLB, 168 μmol/liter cytosol, *versus* LCC, 114 μmol/liter cytosol). These values may be compared with basal and isoproterenol-stimulated data presented above.

PLB knockout simulations were performed to validate with experimental data (Fig. 6*b*) (3). By comparing the magnitude of the calcium transient (systolic calcium concentration) in response to isoproterenol in wild-type controls and PLB knockout models, we assessed the significance of targets other than PLB to the intropic and lusitropic response of the cell to β-adrenergic receptor agonists. This analysis suggests two conclusions. First, it appears that PLB is a dominant but not the sole PKA target responsible for inotropic response. Second, because the model does not include the controversial role of ryanodine receptor phosphorylation or other targets, it is clear that the role of LCC phosphorylation may be sufficient (but not the only contributing source) for the difference between unstimulated and isoproterenol-stimulated PLB knockout models.

DISCUSSION

Although most experimental efforts have focused on small portions of the β-adrenergic signaling network at a time, functionally integrated computational models provide an opportunity to analyze systems properties of whole cell responses. A wealth of past research in β-adrenergic signaling has allowed us to develop and validate a functionally integrated systems model of β-adrenergic signaling, calcium handling, and electrophysiology in the cardiac myocyte. With this systems model, we investigated how the topology and molecular interactions of the β-adrenergic signaling network contribute to the control of excitation-contraction coupling. To accomplish this goal, we performed systematic *in silico* perturbations to the β-adrenergic network, gaining insight into the responses of the network to acute genetic and pharmacologic changes. Systems analysis of such perturbations demonstrated potential in the analysis of molecular therapeutics, experimental design, and identification of signaling control mechanisms.

We began by considering molecular therapeutics, in particular the analysis of potential gene therapies for heart failure. Model analysis not only provided the means to directly compare the effect of receptor overexpression *versus* adenylyl cyclase overexpression, but it also suggested a role for a pharmacological alternative, in which a hypothetical drug is designed to increase the affinity of $G_s\alpha$ and adenylyl cyclase. Whereas the systems model does not reveal how treatments might differ in their ability to affect or be affected by cross-talk with other

non-included pathways (*e.g.* mitogen-activated protein kinase or protein kinase C signaling) and compartmentation, the current model is clearly useful for systematic comparison of targets and identifying design goals and constraints. We found adenylyl cyclase overexpression to be the most sensitive means of increasing agonist-stimulated adenylyl cyclase activity while minimizing changes to basal cyclic AMP content. At the same time, we found evidence for a potential role of pharmacologic agents that may have similar effects to overexpression while obviating the need for gene therapy.

Model analysis often exposes systems properties not readily apparent from examination of a handful of individual experiments. Whereas hypotheses generated using models clearly require testing, the opportunity exists to design experimental protocols *in silico* with which to test these hypotheses. We were surprised to find that whereas adenylyl cyclase appears to be a stoichiometrically limiting step in cyclic AMP synthesis (compared with the large amount of G protein), less than 40% of adenylyl cyclase molecules may be stimulated acutely by G protein under maximally effective isoproterenol concentration. This finding appears to be indirectly supported by previous studies in cardiac myocytes (34). By using the model, we designed a simple protocol using cholera toxin to estimate fractional adenylyl cyclase activation experimentally for any given stimulus, showing that cyclic AMP measured according to the protocol should be linearly proportional to the actual fractional adenylyl cyclase activation. This analysis emphasized the tight range of fractional activation of adenylyl cyclase achieved in physiological situations, bounded on the low end by constitutively activated receptors and bounded on the high end by the number of β-adrenergic receptors able to activate G_s. These results contribute to our basic understanding of amplification mechanisms in cyclic AMP signaling networks.

Although cyclic AMP buffering has been known for many years (26, 36), the functional role it may play has remained unclear. We found that while cyclic AMP buffering by PKA greatly influences the total cyclic AMP content (Fig. 5), basal free cyclic AMP concentration remains much more sensitive to the balance of cyclic AMP synthesis and degradation. The heat-stable PKI, whose functional role is not well characterized, was found in the present study to regulate cyclic AMP buffering and enable ultrasensitivity for PKA activation. From a systems perspective, it appears that PKI may provide additional control over basal cyclic AMP content in the cell at the cost of decreased maximal kinase activity. Thus, cyclic AMP buffering by PKA and its regulation by PKI may have an important role in the control of the basal phosphorylation state of PKA substrate proteins in the cell.

Understanding the quantitative role of numerous phosphorylation targets toward cellular function is important for conceptualizing the fundamental control mechanisms in the cell. We compared the role of L-type calcium channel and phospholamban phosphorylation toward isoproterenol-stimulated changes in calcium handling. Although phosphorylation of both channel and phospholamban contributes significantly to the magnitude of the calcium transient (Fig. 6*a*), other parameters such as lusitropy, diastolic calcium levels, and SR calcium content appear to be dominated by phospholamban phosphorylation. This analysis was further reinforced by the simulation of phospholamban knockouts and their response to isoproterenol. Although other known phosphorylation targets such as troponin I and the ryanodine receptor complex were not included, the current model demonstrates that the major changes to contractility can be accounted for by calcium channel and phospholamban phosphorylation alone.

These studies provide a foundation for a more comprehensive understanding of β-adrenergic control of cardiac myocyte contractility. Future models may include additional PKA targets such as the controversial role of ryanodine receptor phosphorylation (37), troponin I (38), the sarcolemmal Ca^{2+}-ATPase (39), and in the case of species such as rabbit or human, I_{ks} and $I_{Cl(CFTR)}$ (3). Adjustments for heart failure (*i.e.* Na/Ca exchanger up-regulation (21), β-adrenergic receptor down-regulation (40), or PLB gene mutations (41)) would allow insight into the investigation of potential molecular therapeutics. Systems models may also be useful for understanding the physiological roles of signaling cross-talk and compartmentation. We have developed a functionally integrated model of β-adrenergic signaling and control of contractility in the cardiac myocyte, and we have demonstrated the utility of the model as a tool for analysis of molecular therapeutics, experimental design strategies, and control mechanisms fundamental to cellular function. These analyses provide a new systems level perspective for understanding the cardiac myocyte in health and disease.

Acknowledgments—We thank Drs. Jose Puglisi and Donald Bers for generously providing computer code of LabHEART (21) and Dr. Elliot Ross for helpful discussions.

REFERENCES

1. Katz, A. M. (2001) *Physiology of the Heart*, 3rd Ed., pp. 255–352, Lippincott/Williams & Wilkins, New York
2. Bers, D. M. (2002) *Nature* **415,** 198–205
3. Bers, D. M. (2001) *Excitation-Contraction Coupling and Cardiac Contractile Force*, 2nd Ed., pp. 42–282, Kluwer/Academic Publishers, Boston
4. Feldman, A. M. (2002) *Circulation* **105,** 1876–1878
5. Frank, K., and Kranias, E. G. (2000) *Ann. Med.* **32,** 572–578
6. Steinberg, S. F., and Brunton, L. L. (2001) *Annu. Rev. Pharmacol. Toxicol.* **41,** 751–773
7. Xiang, Y., and Kobilka, B. K. (2003) *Science* **300,** 1530–1532
8. Insel, P. A. (2003) *Trends Endocrinol. Metab.* **14,** 100–102
9. Zaccolo, M., and Pozzan, T. (2002) *Science* **295,** 1711–1715
10. Zhang, J., Ma, Y., Taylor, S. S., and Tsien, R. Y. (2001) *Proc. Natl. Acad. Sci. U. S. A.* **98,** 14997–15002
11. Vilardaga, J. P., Bunemann, M., Krasel, C., Castro, M., and Lohse, M. J. (2003) *Nat. Biotechnol.* **21,** 807–812
12. Kamp, T. J., and Hell, J. W. (2000) *Circ. Res.* **87,** 1095–1102
13. Hodgkin, A. L., and Huxley, A. F. (1952) *J. Physiol.* (*Lond.*) **117,** 500–544
14. Noble, D. (2002) *BioEssays* **24,** 1155–1163
15. Gilman, A. G., Simon, M. I., Bourne, H. R., Harris, B. A., Long, R., Ross, E. M., Stull, J. T., Taussig, R., Arkin, A. P., Cobb, M. H., Cyster, J. G., Devreotes, P. N., Ferrell, J. E., Fruman, D., Gold, M., Weiss, A., Berridge, M. J., Cantley, L. C., Catterall, W. A., Coughlin, S. R., Olson, E. N., Smith, T. F., Brugge, J. S., Botstein, D., Dixon, J. E., Hunter, T., Lefkowitz, R. J., Pawson, A. J., Sternberg, P. W., Varmus, H., Subramaniam, S., Sinkovits, R. S., Li, J., Mock, D., Ning, Y., Saunders, B., Sternweis, P. C., Hilgemann, D., Scheuermann, R. H., DeCamp, D., Hsueh, R., Lin, K. M., Ni, Y., Seaman, W. E., Simpson, P. C., O'Connell, T. D., Roach, T., Choi, S., Eversole-Cire, P., Fraser, I., Mumby, M. C., Zhao, Y., Brekken, D., Shu, H., Meyer, T., Chandy, G., Heo, W. D., Liou, J., O'Rourke, N., Verghese, M., Mumby, S. M., Han, H., Brown, H. A., Forrester, J. S., Ivanova, P., Milne, S. B., Casey, P. J., Harden, T. K., Doyle, J., Gray, M. L., Michnick, S., Schmidt, M. A., Toner, M., Tsien, R. Y., Natarajan, M., Ranganathan, R., and Sambrano, G. R. (2002) *Nature* **420,** 703–706
16. Rich, T. C., Fagan, K. A., Tse, T. E., Schaack, J., Cooper, D. M., and Karpen, J. W. (2001) *Proc. Natl. Acad. Sci. U. S. A.* **98,** 13049–13054
17. Bhalla, U. S., and Iyengar, R. (1999) *Science* **283,** 381–387
18. Khalil, H. K. (1996) *Nonlinear Systems*, 2nd Ed., pp. 351–358, Prentice-Hall, Englewood Cliffs, NJ
19. Gao, T., Yatani, A., Dell'Acqua, M. L., Sako, H., Green, S. A., Dascal, N., Scott, J. D., and Hosey, M. M. (1997) *Neuron* **19,** 185–196
20. Luo, C. H., and Rudy, Y. (1994) *Circ. Res.* **74,** 1071–1096
21. Puglisi, J. L., and Bers, D. M. (2001) *Am. J. Physiol.* **281,** C2049–C2060
22. Jafri, M. S., Rice, J. J., and Winslow, R. L. (1998) *Biophys. J.* **74,** 1149–1168
23. Pandit, S. V., Clark, R. B., Giles, W. R., and Demir, S. S. (2001) *Biophys. J.* **81,** 3029–3051
24. Vila Petroff, M. G., Egan, J. M., Wang, X., and Sollott, S. J. (2001) *Circ. Res.* **89,** 445–452
25. Kuznetsov, V., Pak, E., Robinson, R. B., and Steinberg, S. F. (1995) *Circ. Res.* **76,** 40–52
26. Beavo, J. A., Bechtel, P. J., and Krebs, E. G. (1974) *Proc. Natl. Acad. Sci. U. S. A.* **71,** 3580–3583
27. Vittone, L., Mundina-Weilenmann, C., Said, M., and Mattiazzi, A. (1998) *J. Biol. Chem.* **273,** 9804–9811
28. Xiao, R. P., and Lakatta, E. G. (1993) *Circ. Res.* **73,** 286–300
29. Skeberdis, V. A., Jurevicius, J., and Fischmeister, R. (1997) *J. Pharmacol. Exp. Ther.* **283,** 452–461
30. Tepe, N. M., and Liggett, S. B. (1999) *FEBS Lett.* **458,** 236–240
31. Dorn, G. W., II, Tepe, N. M., Lorenz, J. N., Koch, W. J., and Liggett, S. B. (1999) *Proc. Natl. Acad. Sci. U. S. A.* **96,** 6400–6405

32. Hoffmann, A., Levchenko, A., Scott, M. L., and Baltimore, D. (2002) *Science* **298,** 1241–1245
33. Post, S. R., Hilal-Dandan, R., Urasawa, K., Brunton, L. L., and Insel, P. A. (1995) *Biochem. J.* **311,** 75–80
34. Chung, M. K., Gulick, T. S., Rotondo, R. E., Schreiner, G. F., and Lange, L. G. (1990) *Circ. Res.* **67,** 753–763
35. Ferrell, J. E., Jr. (1999) *BioEssays* **21,** 866–870
36. Corbin, J. D., Sugden, P. H., Lincoln, T. M., and Keely, S. L. (1977) *J. Biol. Chem.* **252,** 3854–3861
37. Marks, A. R. (2003) *Circulation* **107,** 1456–1459
38. Konhilas, J. P., Irving, T. C., Wolska, B. M., Jweied, E. E., Martin, A. F., Solaro, R. J., and de Tombe, P. P. (2003) *J. Physiol.* (*Lond.*) **547,** 951–961
39. Dixon, D. A., and Haynes, D. H. (1989) *J. Biol. Chem.* **264,** 13612–13622
40. Koch, W. J., Lefkowitz, R. J., and Rockman, H. A. (2000) *Annu. Rev. Physiol.* **62,** 237–260
41. Schmitt, J. P., Kamisago, M., Asahi, M., Li, G. H., Ahmad, F., Mende, U., Kranias, E. G., MacLennan, D. H., Seidman, J. G., and Seidman, C. E. (2003) *Science* **299,** 1410–1413